Digital Coil: Transmitter Coil with Programmable Radius for Wireless Powering Robust Against Distance Variation

Hao Qiu, Yoshiaki Narusue, Yoshihiro Kawahara, Takayasu Sakurai, and Makoto Takamiya
University of Tokyo, Japan
Email: hqiu@iis.u-tokyo.ac.jp

***Abstract*—A wireless powering system robust against distance variation is required. In this paper, a digital transmitter (TX) coil, whose radius depends on the distance (d) between the TX and receiver (RX) coils, is proposed that maximizes the efficiency of wireless powering. Firstly, we analytically derived the optimum TX coil radius ($r_{TX,\,OPT}$) to maximize the coil-to-coil efficiency (η) by co-optimizing the coupling coefficient and the quality factors of the coils. It was found that $r_{TX,\,OPT}$ was approximately equal to d. Then, a practical implementation of the digital TX coil, whose radius was electrically varied without mechanical motion, was proposed. It was found by a measurement that, compared with a conventional TX coil with a constant radius, the proposed digital TX coil increased η from 12% to 20% when d was four times the RX coil radius.**

***Index Terms*—wireless power transfer, inductive coupling, magnetic resonance, coil-to-coil efficiency, distance variation, coil design, optimum coil radius, 13.56MHz.**

I. Introduction

The efficiency (η_{SYS}) of a wireless power transfer (WPT) system rapidly decreases as the distance (d) between the transmitter (TX) and receiver (RX) coils increases. The most effective way to realize wireless powering robust against d variation is to directly maximize the coil-to-coil efficiency (η). Moreover, the tuning mechanism against d variation should be included on the TX side rather than the RX side, because the RX side should be as simple as possible in, for example, the wireless charging of cellphones. Several wireless powering systems robust against d variations [1-5] have been proposed. In [1-4], impedance matching on both the TX and RX sides of a WPT system was focused on, where η_{SYS} was limited to η. In addition, RX tuning – such as impedance matching between a load impedance and load [1-3] and RX coil layout optimization in [5] – has been proposed but does not satisfy our design target of TX-only tuning. To solve these problems, we proposed a novel digital TX coil with a programmable radius ($r_{TX,\,PROG}$) depending on d, which makes it possible to directly maximize η and thus realize a system with η_{SYS} robust against d variation. Additionally, the digital TX coil uses TX-only tuning. Throughout this work, we focus on η.

Fig. 1 shows the key concept of this paper. Fig. 1 (a) shows a conventional TX coil with a constant radius and the proposed TX coil with $r_{TX,\,PROG}$, which depends on d ($r_{TX,\,PROG}$=d). Fig. 1 (b) shows a schematic diagram of the d dependence of η. When d is increased from d_1 to d_2, the proposed TX coil has a higher η for d_2 than the conventional TX coil.

In Section II, an optimum TX coil radius is derived analytically, by o-optimization of the TX-to-RX coupling coefficient (k) and the quality factors of the coils, and it is found to be approximately equal to d. This is then confirmed by electromagnetic simulation and coil-to-coil measurement. Then, as reported in Section III, the proposed digital TX coil with $r_{TX,\,PROG}$ is fabricated and measured.

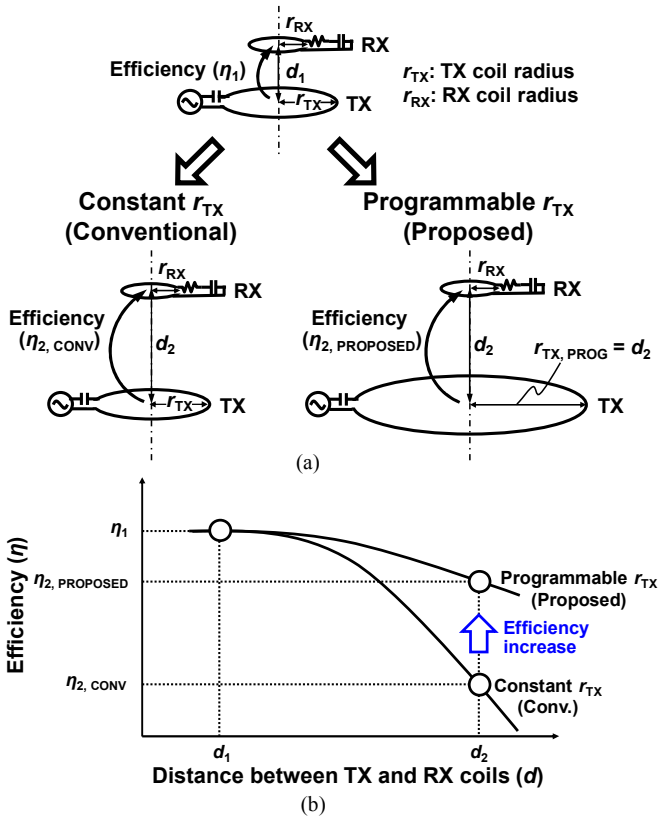

Fig. 1. Key concept of this paper. (a) Conventional TX coil with constant radius and proposed TX coil with $r_{TX,\,PROG}$. Here, single-turn coil is plotted for simplicity. (b) Schematic diagram of d dependence of η.

II. Optimum TX Coil Radius for Maximum Efficiency

A. Derivation of Equation

We first analytically derived the optimum TX coil radius for the maximum η under the condition that the RX coil radius (r_{RX}) is much smaller than that of the TX coil (r_{TX}). In WPT systems, η depends on the quality factors of the TX (Q_{TX}) and RX (Q_{RX}) coils and k, a combination of which ($k^2Q_{TX}Q_{RX}$) must be maximized at the resonance frequency (f_0) to maximize η [6]:

978-1-5386-5159-9/18/$31.00 ©2018 IEEE

$$k^2 Q_{TX} Q_{RX} = (\sigma A f_0)^2 \frac{1}{mn} \frac{M^2}{r_{TX} r_{RX}}. \quad (1)$$

Here, σ is the conductivity of the coil metal, A is the cross-sectional area of the current flow in the metal considering skin effects, and M is the mutual inductance between the TX and RX coils. m and n are the numbers of turns of the TX and RX coils, respectively. Here, the increase in resistance due to proximity effects between different turns is neglected.

Using Maxwell's equations, M can be obtained as [7]

$$M = \mu_0 mn \sqrt{r_{TX} r_{RX}} \left[\left(\frac{2}{\beta} - \beta \right) K - \frac{2}{\beta} E \right] \quad (2)$$

$$\beta = \frac{2\sqrt{r_{TX} r_{RX}}}{\sqrt{d^2 + (r_{TX} + r_{RX})^2}}, \quad (3)$$

where μ_0 is the permeability and the complete elliptic integrals are $K = \int_0^{\pi/2} d\theta / \sqrt{1 - k^2 \sin^2\theta}$ and $E = \int_0^{\pi/2} d\theta \sqrt{1 - k^2 \sin^2\theta}$. Here, the physical thicknesses of both the TX and RX coils are assumed to be zero.

For $r_{RX} << r_{TX}$, M in (2) can be approximated as

$$M_0 = \frac{\mu_0 \pi}{2} mn \frac{r_{TX}^2 r_{RX}^2}{(d^2 + r_{TX}^2)^{3/2}}. \quad (4)$$

Then, $k^2 Q_{TX} Q_{RX}$ in (1) can be simplified as

$$k^2 Q_{TX} Q_{RX} = \left(\frac{\mu_0 \pi \sigma A f_0}{2}\right)^2 mn r_{RX}^3 \frac{1}{(r_{TX} + d^2 / r_{TX})^3}. \quad (5)$$

Note that when all other parameters (f_0, m, n, r_{RX}, d) are constants, $k^2 Q_{TX} Q_{RX}$ in (5) reaches at its maximum value, which also corresponds to the maximum η, if and only if r_{TX} is at its optimum value ($r_{TX,\,OPT}$) of

$$r_{TX,\,OPT} = d. \quad (6)$$

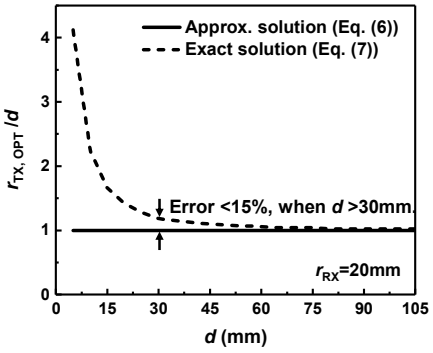

Fig. 2. d dependence of $r_{TX,\,OPT}$ normalized by d showing approximate and exact solutions.

In addition, the error introduced in (4) is estimated. Instead of using (4) for the mutual inductance, (2) is substituted into (1) and $r_{TX,\,OPT}$ can be obtained by solving

$$\frac{\partial}{\partial r_{TX}} k^2 Q_{TX} Q_{RX} = 0. \quad (7)$$

Here, we set f_0=13.56MHz, m=5, n=3, and r_{RX}=20mm. Fig. 2 shows a comparison between $r_{TX,\,OPT}$ in its approximate form [$r_{TX,\,OPT}$(approx.)] and its exact solution [$r_{TX,\,OPT}$(exact)]. According to Fig. 2, $r_{TX,\,OPT}$(approx.) deviates from $r_{TX,\,OPT}$(exact) at a small d, while they converge at a large d. The percentage error decays rapidly as d increases and thus (6) gives a reasonable approximation with error<15% from (7) for d>30mm.

B. Validation by Electromagnetic Simulation

To confirm that (6) is a good guideline for TX coil design in WPT systems, electromagnetic simulation software (EMPro, Keysight Technologies) was used. Table I summarizes the design specifications of both the TX and RX coils. f_0 was finely tuned to 13.56MHz for both coils using compensation capacitors. Considering the physical thickness of the coils, d is defined as the distance from the geometrical center point of the TX coil to that of the RX coil.

Fig. 3 shows the simulated relationship of η versus r_{TX} for different d. As expected, η is maximized at $r_{TX,\,OPT}$, although it deviates from (6). The deviation is ascribed to the simplified assumptions made in the analysis. Considering that the electromagnetic simulation gives more accurate results than equation analysis, in this work, we set $r_{TX,\,OPT}$ as 35mm, 45mm, 70mm, and 80mm for d of 35mm, 50mm, 65mm, and 80mm, respectively. However, it is emphasized that (6) still acts as a good design guideline with a tolerable percentage error (<12%).

TABLE I

DESIGN SPECIFICATIONS OF TX AND RX COILS

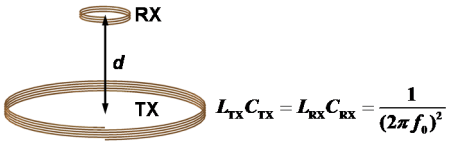

Design specifications	TX Coil	RX Coil
f_0 (MHz)	13.56	
Metal material	Cu	
Metal wire diameter (mm)	1	
Radius (mm)	r_{TX}	20
Number of turns	5	3
Metal wire pitch (mm)	2	

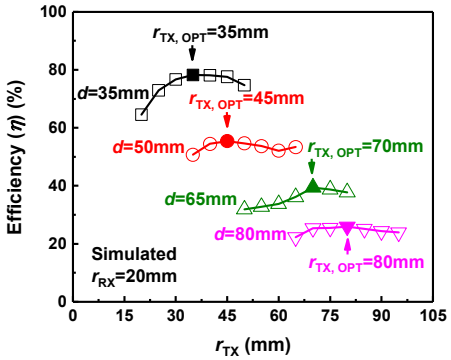

Fig. 3. Simulated η vs r_{TX} for different d.

Fig. 4 shows the simulated relationship of η versus d for conventional and proposed programmable TX coils with the same RX coil. As can be seen, compared with the conventional TX coil, the proposed coil with $r_{TX,\,OPT}$ has a maximum η for different d. For example, for d=80mm, η is 10% using the TX coil with r_{TX}=35mm but is increased to 26% (more than doubled) when the TX coil with $r_{TX,\,OPT}$=80mm is used. Similarly, for

d=35mm, η is 63% using the TX coil with r_{TX}=80mm but is increased to 78% when the TX coil with $r_{TX,\,OPT}$=35mm is used.

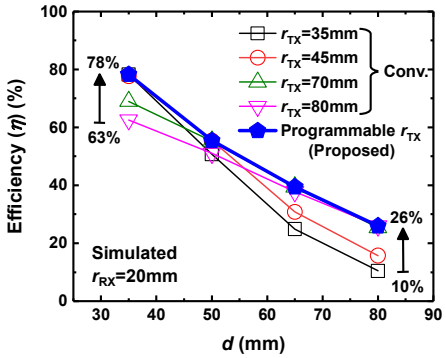

Fig. 4. Simulated η vs d using TX coil with conventional constant r_{TX} and proposed $r_{TX,\,PROG}$.

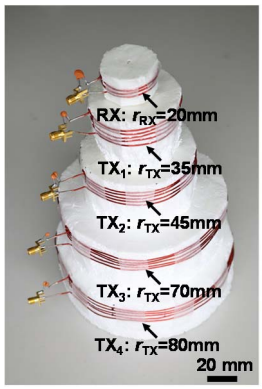

Fig. 5. Fabricated TX coils with r_{TX} of 35mm, 45mm, 70mm, and 80mm. r_{RX} is 20mm.

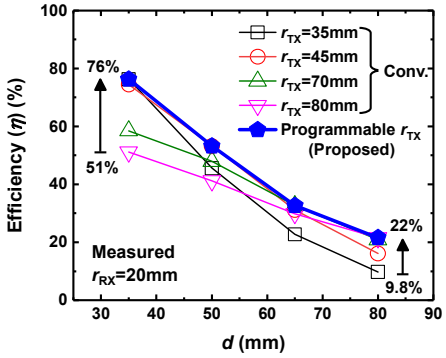

Fig. 6. Measured η vs d using TX coils in Fig. 5.

C. Experimental Validation

In addition, measurements were performed for comparison with the simulation results. As shown in Fig. 5, four TX coils (TX_1: r_{TX}=35mm; TX_2: r_{TX}=45mm; TX_3: r_{TX}=70mm; TX_4: r_{TX}=80mm) and an RX coil (r_{RX}=20mm) were fabricated according to the design specifications in Table I. f_0 was finely tuned to 13.60MHz for all coils using compensation capacitors. A network analyzer (E5061B, Keysight Technologies) was used to measure the S parameter for each pair of the TX and RX coils, and η was calculated as $|S_{21}|^2/(1-|S_{11}|^2)$. Fig. 6 shows the measured relationship of η versus d for different TX coils with the same RX coil. Compared with the simulation results in Fig. 4, the absolute value of η is slightly lower, which is reasonable considering the mismatch between the simulated and fabricated coils. Note that a similar conclusion can be arrived at from the fact that the proposed programmable TX coil with $r_{TX,\,OPT}$ has a maximum η for different d. Taking d=80mm as an example, η is 9.8% using the TX coil with r_{TX}=35mm but is increased to 22% (still more than doubled) when the TX coil with $r_{TX,\,OPT}$=80mm is used.

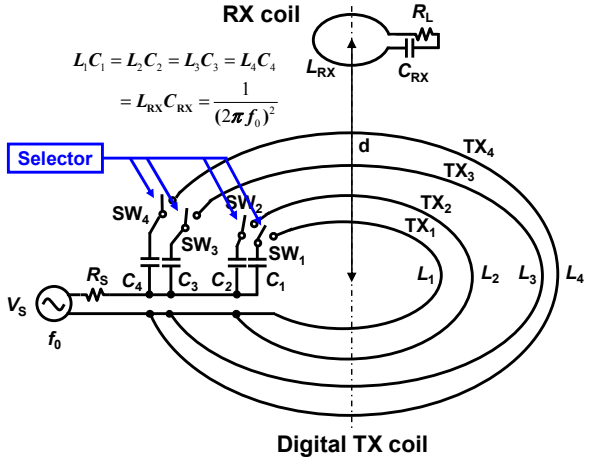

Fig. 7. Schematic of the proposed digital TX coil, in which one of four sub-coils with different radii is selectively turned on depending on d. Here, single-turn coil is plotted for simplicity.

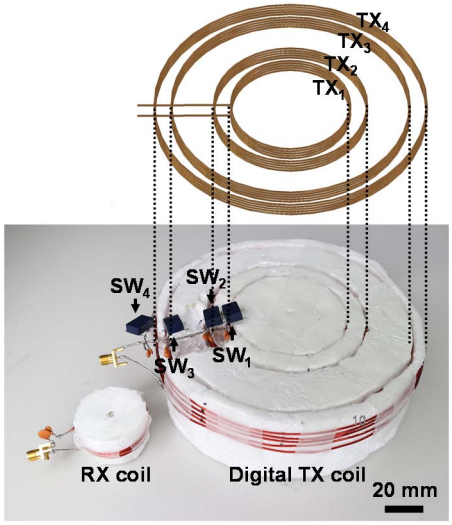

Fig. 8. Fabricated digital TX and RX coils.

III. Proposed Digital TX Coil

On the basis of the above analysis, the TX coil with $r_{TX,\,PROG}$ designed according to (6) can alleviate η degradation with d variation. However, its practical implementation is still an issue. Rather than using motors to mechanically change r_{TX} for the TX coil, we propose the use of switches to electronically program r_{TX}. As shown in Fig. 7, the proposed digital TX coil is composed of four concentric sub-coils (TX_1, TX_2, TX_3, and TX_4), four compensation capacitors, and four switches (SWs).

Each sub-coil resonates at the same f_0 as the RX coil. The selector is used to control these four SWs. For each d, only the sub-coil with $r_{TX,\,OPT}$ that can achieve the maximum η is turned on by the selector. For example, when d is 80mm, TX_4 with r_{TX}=80mm is turned on by selecting SW_4. Fig. 8 shows a photograph of the digital TX coil, which was fabricated from the four TX coils in Fig. 5. The geometric structure of the digital TX coil is also given. The compensation capacitors were also reselected to tune f_0 for each sub-coil to 13.60MHz. Here, a relay (Panasonic Electric Works TQ2-L2-4.5) with an ON resistance of less than 50mΩ was used for each SW.

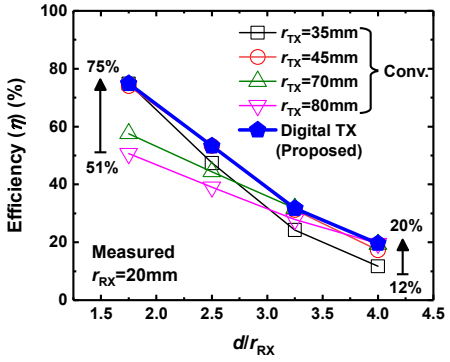

Fig. 9. Measured η vs d/r_{RX} using digital TX coil in Fig. 8.

Fig. 9 shows the measured relationship of η versus d normalized by r_{RX} (d/r_{RX}). As highlighted in blue, the proposed digital TX coil provides the maximum η by selectively turning on TX_1, TX_2, TX_3, and TX_4 when d equals 1.75, 2.5, 3.25, and 4 times r_{RX}, respectively. Taking d=r_{RX}×4 as an example, η can be improved from 12% to 20% by selectively turning on TX_4 rather than TX_1. In addition, η can be improved from 51% to 75% at d=r_{RX}×1.75, when TX_1 rather than TX_4 is turned on.

Here, we further discuss the proposed digital TX coil. Firstly, the coupling from the other three unselected open sub-coils in the proposed digital TX coil may cause η degradation [6]. However, by comparing Figs. 6 and 9, η only shows a minor fluctuation of ±2%, which means that the effect of such coupling is negligible. Secondly, one of the four sub-coils in the digital TX coil was manually selected according to d in this paper. In our future work, however, an RX localization subsystem, based on which r_{TX} can be automatically programmed, will be implemented to establish an advanced WPT system. Finally, in this work, only the ideal scenario has been discussed, in which the RX coil is always concentrically aligned with the TX coil and only d is changed. In real applications, however, it is not uncommon for the RX coil to be misaligned with the TX coil. Although the discussion of this is beyond the scope of this work, the digital TX coil with $r_{TX,\,PROG}$, whose optimum value will deviate from (6), is still promising for alleviating η degradation.

Table II shows a comparison of the proposed digital TX coil with previously reported WPT systems robust against d variation. Only the proposed system achieved both coil-to-coil efficiency maximization and TX-only tuning, making it practical for wireless powering robust against d variation in real applications (e.g., the wireless charging of cellphones).

TABLE II
COMPARISON WITH PREVIOUSLY REPORTED WPT SYSTEMS ROBUST AGAINST DISTANCE VARIATION

Ref.	Coil-to-coil efficiency maximization	TX-only tuning
[1]	No	No
[2]	No	No
[3]	No	No
[4]	No	Yes ✔
[5]	Yes ✔	No
This work	Yes ✔	Yes ✔

IV. CONCLUSION

In this paper, a digital TX coil, whose radius was optimized according to d, was proposed to maximize system efficiency in WPT systems when an RX coil is given. Firstly, by co-optimization of both the coupling coefficient and the quality factors of the coils, we derived the relationship between the optimum TX coil radius and d. These two values were approximately equal for a maximum coil-to-coil efficiency. In addition, a practical implementation of the digital TX coil using relay switches to selectively turn on one of the four sub-coils was proposed. Compared with a conventional system without the proposed coil, experimental results showed an increase in coil-to-coil efficiency from 12% to 20% at d of four times the RX coil radius. Also, in contrast to previously reported systems, the proposed digital TX coil maximizes coil-to-coil efficiency and thus realizes a value of system efficiency robust against d variation. Moreover, no tuning in RX is required.

ACKNOWLEDGMENT

This work was partially supported by JST ERATO Grant Number JPMJER1501, Japan.

REFERENCES

[1] T. P. Duong and J.-W. Lee, "Experimental results of high-efficiency resonant coupling wireless power transfer using a variable coupling method," *IEEE Microw. Wirel. Compon. Lett.*, vol. 21, no. 8, pp. 442-444, Aug. 2011.

[2] J. Kim and J. Jeong, "Range-adaptive wireless power transfer using multiloop and tunable matching techniques," *IEEE Trans. Ind. Electron.*, vol. 62, no. 10, pp. 6233-6241, Oct. 2015.

[3] B.-C. Park and J.-H. Lee, "Adaptive impedance matching of wireless power transmission using multi-loop feed with single operating frequency," *IEEE Trans. Antennas Propag.*, vol. 62, no. 5, pp. 2851-2856, May. 2014.

[4] G. Lee, B. H. Waters, Y. G. Shin, J. R. Smith, and W. S. Park, "A reconfigurable resonant coil for range adaption wireless power transfer," *IEEE Trans. Microw. Theory Tech.*, vol. 64, no. 2, p. 624-632, Feb. 2016.

[5] S. B. Lee and I. G. Jang, "Layout optimization of the secondary coils for wireless power transfer systems," in *2015 IEEE Wireless Power Transfer Conf.*, 2015.

[6] U.-M. Jow and M. Ghovanloo, "Geometrical design of a scalable overlapping planar spiral coil array to generate a homogeneous magnetic field," *IEEE Trans. Magn.*, vol. 49, no. 6, pp. 2933-2945, Jun. 2013.

[7] S. Ramo, J. R. Whinnery, and T. Van Duzer, *Fields and Waves in Communication Electronics*, 3rd ed., New York. John Wiley & Sons Inc., 2007.